Concentrational effects in anisotropic artificial Kerr media

J. C. Kralik, B. E. Vugmeister, and M. S. Malcuit
Department of Physics, Lehigh University, 16 Memorial Drive East, Bethlehem, Pennsylvania 18015-3182
(Received 29 July 1994)

We report the results of experimental and theoretical studies of the laser-induced birefrigence of concentrated suspensions of shaped, anisotropic artificial Kerr media. The systems we investigate experimentally are aqueous suspensions of polytetrafluoroethylene (PTFE). The observed slowing down of the relaxation of the birefringence signal is in agreement with pretransitional behavior near the isotropic-nematic phase transition. However, in order to explain the relatively small increase of the induced birefringence with an increase in concentration, and the double exponential character of relaxation, one should include the possible deviation of the optical axis from the geometrical, or long, axis of the PTFE particles.

PACS number(s): 42.65.Vh

I. INTRODUCTION

Dilute, anisotropic artificial Kerr media (AAKM) have attracted much attention in recent years because of their potential for applications in nonlinear optics such as switching [1], phase conjugation by degenerate four-wave mixing [2], and coherent beam combining [3,4]. This class of materials is comprised of suspensions of optically anisotropic dielectric microparticles, which develop an induced dipole moment in the presence of an applied electric field. These dipoles in turn interact with the applied field generating an electrostrictive torque, which tends to align the axis of the particle with highest polarizability (the optical axis) along the applied field direction. The field-induced reorientations of the particles makes the system anisotropic and birefringent.

The majority of experimental and theoretical investigations of the nonlinear optical properties of AAKM have utilized dilute suspensions of microparticles. However, one could expect that for relatively long particles, laser-induced ordering, and hence, laser-induced birefringence, increases dramatically with increasing particle concentration due to excluded-volume effects. Excluded-volume effects could eventually cause spontaneous, nematic ordering; a well-known phenomenon in liquid crystals [5]. Pretransitional, orientational ordering in polytetrafluoroethylene (PTFE) has been observed recently in an investigation of birefringence induced by shear flow [6].

The investigation of the concentrational effects in laser-induced birefringence is the subject of the present paper [7]. It was found that the pretransitional behavior of the orientational order parameter was suppressed and that the relaxation of the orientational ordering does not decay exponentially. These results are explained by the noncoincidence of the optical and geometrical axes of the PTFE particles.

II. THEORETICAL BACKGROUND

The commonly used model of an AAKM is a suspension of cylindrically symmetric, uniformly sized, optically anisotropic rigid rods whose long axis is colinear with the optical axis. The suspension is placed in a spatially uniform, linearly polarized, oscillating electric field whose frequency of oscillation is much faster than the reorientational relaxation time of the particles.

The orientational order parameter of the AAKM is written as follows:

$$S=\tfrac{1}{2}\int d\Omega\,\Psi(\theta)(3\cos^2\theta-1)\ , \tag{1}$$

where θ is the angle between the field direction and the long axis of a particle and $\Psi(\theta)$ is the distribution function of particle orientations. In equilibrium, the distribution function is the normalized Boltzmann distribution

$$\Psi(\theta)=\frac{\exp[-U/kT]}{\int d\Omega\exp[-U/kT]}\ , \tag{2}$$

where the potential energy is the sum of both electrostrictive and excluded-volume contributions: $U=U_E+U_{\rm ex}$. The electrostrictive potential energy is given by [8]

$$U_E=-\frac{\beta}{2}\bar{E}^2\cos^2\theta\ , \tag{3}$$

where $\beta=\alpha_\parallel-\alpha_\perp$ is the polarizability anisotropy of the particles, E is the time-varying electric field, and the overbar represents a time average over the period of the oscillating electric field. To take into account the effect of particle-particle interactions, the mean-field approximation is used to write the *effective* excluded-volume potential [9]

$$U_{\rm ex}=-\tfrac{3}{2}mk_BT(\cos^2\theta-\tfrac{1}{3})S\ . \tag{4}$$

Here, m is a dimensionless parameter proportional to the product of the particle-number density N_0 and the excluded volume per particle $V_{\rm ex}$, and will be referred to as the relative concentration of the AAKM. By substituting Eqs. (2), (3), and (4) into Eq. (1), a self-consistent equation for the order parameter is obtained,

$$S=\frac{\frac{3}{2}\int_0^{\pi}d\theta\sin\theta(\cos^2\theta-1/3)\exp[(\frac{3}{2}mS+J)\cos^2\theta]}{\int_0^{\pi}d\theta\sin\theta\exp[(\frac{3}{2}mS+J)\cos^2\theta]}, \tag{5}$$

where

$$J=\frac{\beta\bar{E}^2}{2k_BT} \tag{6}$$

will be referred to as the intensity parameter.

The numerical solution of Eq. (5) is presented in Fig. 1 in the (S,J) plane. The orientational order depends on two control parameters: m and J. In the absence of fields ($J=0$), the system undergoes a first-order phase transition at the relative critical concentration $m=m_c=4.486$. At that point, the system spontaneously separates into coexisting isotropic and nematic phases. When the concentration is near the critical concentration (i.e., $m\approx4.3$), small fields corresponding to $J\approx0.08$ are enough to observe a nonequilibrium phase transition, or switching, from the paranematic state where $S\ll1$ to the nematic state where $S\approx1$. Take note also that dashed lines in Fig. 1 indicate places where $\partial S/\partial J<0$, which are unstable solutions of S. Because of this, the system exhibits hysteresis over the concentration range of $4.3<m<4.486$. This range represents a 2% variation in concentration, and therefore for the hysteresis to be observed, the volume fraction of particles needs to be controlled to better than 2%. Finally, the model predicts that at a relative concentration of $m^*=5$ (not shown in Fig. 1), the isotropic phase becomes unstable.

After turning off the field, the relaxation of the order parameter to the equilibrium isotropic state in mean-field theory is given by the following master equation:

$$\frac{dS}{dt}=-\frac{1}{\tau}(S-S^{eq}). \tag{7}$$

Here $S(t)$ is the time-varying orientational order parameter, τ is the reorientational time for noninteracting particles, and $S^{eq}(S)$ is the quasiequilibrium order parameter, whose functional form is given by the right-hand side of Eq. (5). For small S, S^{eq} may be expanded in a power series in S, keeping only terms linear in S. Equation (7) then becomes

$$\frac{dS}{dt}=-\frac{1}{\tau^*}S, \tag{8}$$

where

$$\frac{1}{\tau^*}=\frac{1}{\tau}\left[1-\left[\frac{\partial S^{eq}}{\partial S}\right]_{S=0}\right]=\frac{1}{\tau}\left[1-\frac{m}{m^*}\right]=\frac{1}{\tau}\left[1-\frac{\phi}{\phi^*}\right], \tag{9}$$

and where ϕ is the volume fraction of microparticles and ϕ^* is the volume fraction corresponding to the relative concentration m^*. Hence the reorientational relaxation time is seen to diverge as the concentration of the AAKM approaches ϕ^*, which is a typical feature of phase transitions near the instability point.

To reiterate the important results of this section, field-induced switching of the orientational order parameter should take place for concentrated suspensions of shaped microparticles for very modest intensity parameters. As a numerical example, consider the shaped AAKM utilized in Refs. [1–4] which is an aqueous suspension of roughly 2:1 aspect ratio PTFE particles. The polarizability anisotropy of these particles was measured to be $\beta=7\times10^{-17}$ cm^3 [10], and therefore the field intensity necessary to observe switching of the order parameter (i.e., for $J=0.08$) is only 30 kW/cm^2 at concentrations corresponding to $m=4.3$. This intensity is easily attainable by focusing the output of 1-W cw argon ion or Nd:YAG (neodymium-doped yttrium aluminum garnet) lasers. The prospect of switching the orientational order parameter, and hence the index of refraction, of concentrated AAKM at such low electric-field intensities offers the same exciting prospects for nonlinear optics as are available by using the related material system of thermotropic nematic liquid crystals [11].

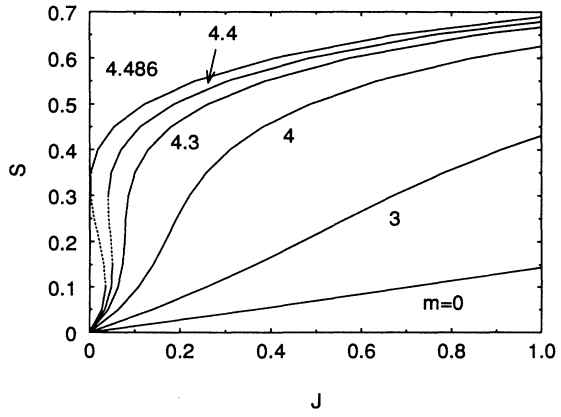

FIG. 1. Orientational order parameter versus intensity parameter for several values of the relative concentration m, calculated using Eq. (5).

III. EXPERIMENT

A. Laser-induced birefringence

In order to experimentally examine the role of excluded-volume effects on the orientational ordering of shaped AAKM, we studied two aqueous suspensions of PTFE. One suspension contains particles with semimajor and semiminor axes of $a=200\pm20$ nm, $b=82\pm8$ nm, or an aspect ratio (AR) of 2.4:1 [12], while the other has $a=150\pm15$ nm, $b=110\pm11$ nm, or an AR of 1.4:1 [13]. These dimensions were determined by transmission electron microscopy of dried samples. The 1.4:1 AR particles were included in this work to serve as a control sample; manifestations of excluded-volume effects are not expected on their orientational ordering since these particles are nearly spherical. In both samples, the particles possess a degree of crystallinity and are birefringent; the higher index of refraction is believed to be along the long

axis of the particles [14]. Values of the intrinsic birefringence Δn_{int} measured for PTFE particles similar to the ones used here range over $\Delta n_{\text{int}}=0.023-0.064$ [14,15]. It is the intrinsic birefringence, rather than the shape, of the PTFE samples utilized here and in Refs. [14,15] that contributes most to the anisotropy in polarizability [14]. The average index of refraction of PTFE is 1.376 [15,16].

We used an optical Kerr experiment to study excluded-volume effects on the orientational ordering in PTFE suspensions; a schematic diagram of the experiment is shown in Fig. 2. A linearly polarized cw argon-ion laser operating at 514.5 nm is focused by lens $L2$ to a spot size of 25 μm in a sample cell; this laser is mechanically chopped (CH) to facilitate temporal measurements. A 5-mW He-Ne probe laser is focused by lens $L1$ to a spot size of 22 μm at the sample cell, and is polarized at 45° with respect to the pump laser field by a polarizing beam splitter (PBS1). The analyzer (PBS2) is another polarizing beam splitter with its transmission axis oriented at 90° to that of PBS1. The transmitted probe light is detected by a Hamamatsu 1P28A photomultiplier tube (PMT). A waveplate (WP) is inserted in the probe beam path between the two crossed polarizers in order to compensate for stress birefringence in the focusing lenses and sample cell.

The probe intensity that reaches the detector is given by

$$I(L)=I(0)\sin^2\left[\frac{\pi\Delta n_{\text{LIB}}L}{\lambda_0}\right], \tag{10}$$

where $I(0)$ is the incident probe intensity, Δn_{LIB} is the laser-induced birefringence of the suspension, L is the sample length, and λ_0 is the wavelength of the probe light in vacuum. If the pump laser intensity has a value such that $J\ll 1$, and the suspension is dilute, the laser-induced birefringence can be expressed as [17]

$$\Delta n_{\text{LIB}}=\frac{8\pi^2}{15n_h^2c}\frac{N_0\beta^2 I_{\text{pump}}}{k_BT}, \tag{11}$$

where n_h is the host fluid index of refraction, c is the speed of light, N_0 is the particle number density, and $I_{\text{pump}}=(n_hc/2\pi)|E|^2$ is the pump laser intensity (cgs units). Using Eqs. (10) and (11) the polarizability anisotropies β were measured for both samples. Figure 3 shows the laser-induced birefringence versus pump intensity for dilute suspensions of both the 2.4:1 and 1.4:1 AR particles. The data show both that the induced birefringence is linearly dependent on I_{pump} and that the slopes of the best-fit lines through the data scale linearly with concentration, as predicted by Eq. (11). Utilizing the average of the slopes of the three best-fit lines shown in Fig. 3, the calculated polarizability anisotropies of the two samples are $\beta=6.2\times10^{-17}$ cm^3 for the 2.4:1 AR particles and $\beta=5.8\times10^{-17}$ cm^3 for the 1.4:1 AR particles. These measured values of β are used to express the pump laser intensity in terms of J.

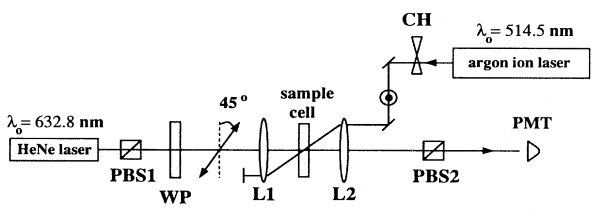

FIG. 2. Schematic diagram of the optical Kerr experiment; see text for a detailed description of the components.

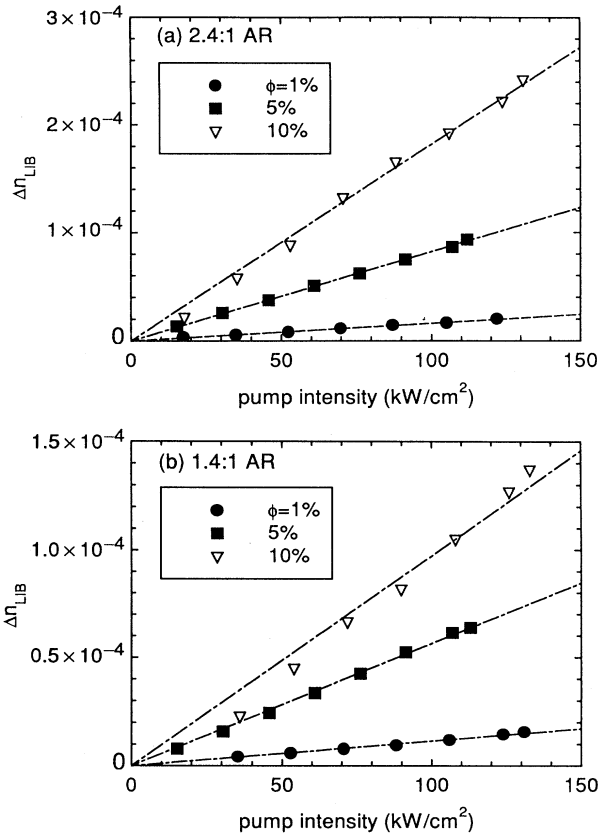

FIG. 3. Laser-induced birefringence versus pump intensity for several dilute suspensions of the (a) 2.4:1 AR and (b) 1.4:1 AR PTFE particles. The dashed lines are the best-fit linear functions to the data.

To calculate the orientational order parameter from the measured induced birefringence, the following general formula is used [17]:

$$\Delta n_{\text{LIB}}=\frac{2\pi\phi}{n_h}\frac{\beta}{v}S\approx\phi\Delta n_{\text{int}}S, \tag{12}$$

where v is the volume per particle. [The last approximation in Eq. (12) is valid if the two indices of refraction of the microparticle are not very different from the host index, as is the case for PTFE in water.] Using Eq. (12) and the experimentally determined values of β, the two intrinsic birefringence values were found to be $\Delta n_{\text{int}}=0.052$ (2.4:1 AR) and $\Delta n_{\text{int}}=0.036$ (1.4:1 AR); these values fall well within the range of values quoted earlier.

Figure 4 presents the experimentally determined orientational order parameter versus intensity parameter for

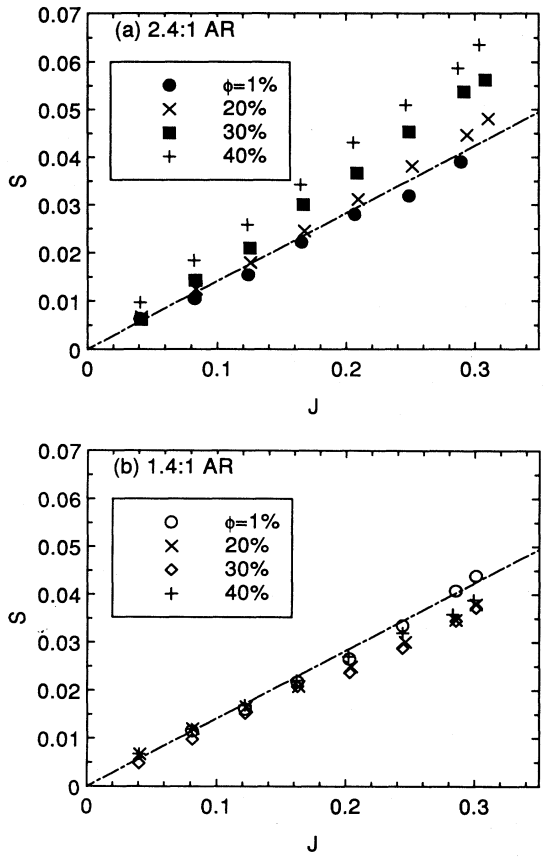

FIG. 4. Orientational order parameter versus intensity parameter at various concentrations for (a) 2.4:1 AR and (b) 1.4:1 AR particles. The dashed lines are the solutions of Eq. (5) when $m=0$.

both samples at four representative concentrations. The dashed line in each graph is the $m=0$ curve from Fig. 1; this curve compares well with the data at the lowest concentrations. It is evident that the order parameter increases with increasing concentration at a given value of the pump intensity for the 2.4:1 AR particles, while the order parameter for the 1.4:1 AR particles does *not* depend on concentration. We attribute the increase in order parameter with concentration for the 2.4:1 AR particles at constant pump intensity to excluded-volume effects. However, the increase in order parameter is much less than one might have expected, based on Fig. 1. Although we do not know the exact relationship between m and ϕ, an estimation can be made. It was observed that the stock solution at $\phi=40\%$ did *not* spontaneously separate into coexisting isotropic and nematic phases. This was determined by observing that filled sample cells placed between crossed polarizers remained uniformly dark when backlit by an extended white light source. If any portion of the suspension had been in the nematic phase, light would have been able to pass through the crossed polarizers. This test showed that $\phi=40\%$ corresponds to $m<m_c=4.486$, thus providing an upper limit for m.

B. Birefringence induced by a low-frequency E field

In order to confirm the unexpectedly low increase of the orientational order parameter with increasing concentration in the laser-induced birefringence experiment, we performed an *electric birefringence* (EB) experiment utilizing a low-frequency electric field, which allowed the range of J to be extended to arbitrarily large values. The experimental setup for the EB measurement is identical to that employed for the optical Kerr measurement (Fig. 2), except that in the EB experiment, the strong, polarized field used to align the microparticles is a 20-kHz electric field generated by an electrode pair similar in design to the one described in Ref. [18]. A problem associated with using a low-frequency electric field to align microparticles in the samples used in this work is that free ions in the aqueous PTFE suspensions can migrate in the water under the influence of the applied field so as to produce a dipole moment, which cancels the induced dipole of the microparticle [19]. We were able to overcome this problem by cleaning the stock PTFE suspension by dialysis. A rough estimate of the electric-field strength between the electrodes of our cell is $E\sim 10$ kV_{rms}/cm. This value is roughly the same as the maximum pump laser electric-field amplitude in the optical Kerr experiment of 40 kV/cm; however, higher values of the intensity parameter J can be achieved in the EB experiment than in the optical Kerr experiment, because the polarizability anisotropy of the particles β is about 100 times greater when using low-frequency electric fields than at optical frequencies [10].

The order parameter versus the square of the applied electrode voltage V_{elec} is plotted in Fig. 5 for several concentrations of the 2.4:1 AR particles. Due to the fact that the value of β was not known precisely, the abscissa in Fig. 5 is labeled in terms of the electrode voltage, rather than in terms of J. It is evident from these data that, although the intensity parameter J is high enough to saturate the rotational degree of freedom of the particles, the basic conclusion is the same as that obtained from the

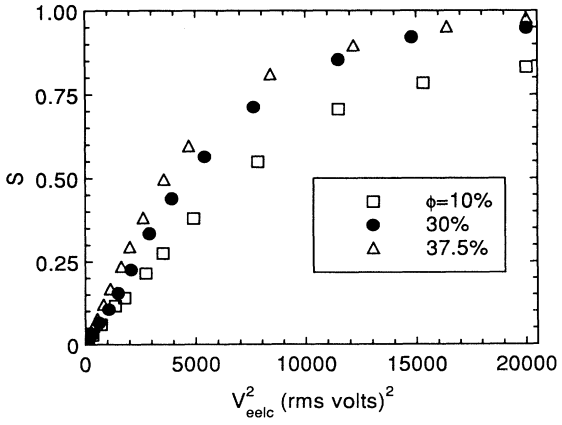

FIG. 5. Measured orientational order parameter versus the square of the applied electrode voltage from the electric birefringence experiment.

optical Kerr experiment: concentrational effects are relatively small in this system.

C. Relaxation time

The relaxation time of the orientational order parameter was measured as a function of particle concentration in the optical Kerr experiment by recording the decay of the transmitted probe intensity after the pump laser is chopped off. Experimentally, we find that for the 2.4:1 AR particles at the higher concentrations, the relaxation of the order parameter cannot be described by a single exponential function. We fit the decay of the order parameter to the sum of two exponential functions rather than a single exponential function as prescribed by Eq. (8). The justification for this choice will be discussed in the next section. More precisely, the decay of the order parameter is fit to

$$\frac{S(t)}{S(0)} = c_f \exp(-t/\tau_f) + c_s \exp(-t/\tau_s) , \tag{13}$$

where $\tau_{f,s}$ are fast and slow reorientational relaxation time constants and $c_{f,s}$ are the weights of the fast and slow components, with $c_f = c_s = 1$. In Fig. 6, the time dependence of the order parameter is displayed for two concentrations of the 2.4:1 AR particles; the dashed curves in the figure are the fits of Eq. (13) to the data. It was observed that for the 1.4:1 AR particles at all concentrations investigated and for the 2.4:1 AR particles, for concentrations less than 30%, the relaxation process could be adequately described with a single relaxation rate. However, as is evident in Fig. 6(b), the higher concentrations of the 2.4:1 AR particles exhibit two time scales during relaxation.

Figure 7 displays the relaxation-time constants as a function of concentration for both samples studied. The 2.4:1 AR sample develops two relaxation-time constants as concentration increases; the fast time constant is relatively independent of concentration, while the slow one diverges as the concentration increases. The solid line in Fig. 7 is a fit of the slow time constant data using the equation

$$\tau_s = \frac{\tau_f}{1-\phi/\phi^*} . \tag{14}$$

This fit yields a value for ϕ^* of 44%. The weight for the fast component, averaged over the data corresponding to $\phi \geq 30\%$, is $\bar{c}_f = 0.174 \pm 0.008$; therefore, the weight of the slow component is $1-\bar{c}_f = \bar{c}_s = 0.826 \pm 0.008$. Thus the dominant relaxation process for concentrations greater than 30% is the slow one, which implies that collective effects play the dominant role in the decay of the orientational order. In contrast to the relaxation times of the 2.4:1 AR particles, the relaxation time constant for the 1.4:1 AR particles is seen to be relatively independent of concentration, which is similar in behavior to the fast time constant of the 2.4:1 AR particles. Thus it is clear from the data in Fig. 7 that the relaxation time is a strong function of the shape of the particle, since it grows by more than a factor of 45 for the 2.4:1 AR particles, while that of the 1.4:1 AR particles grows by only a factor of 5.

IV. TWO COUPLED ORDER PARAMETERS

To summarize the results of the optical Kerr and EB experiments using the 2.4:1 AR particles, the observed divergence of the reorientational relaxation time is basi-

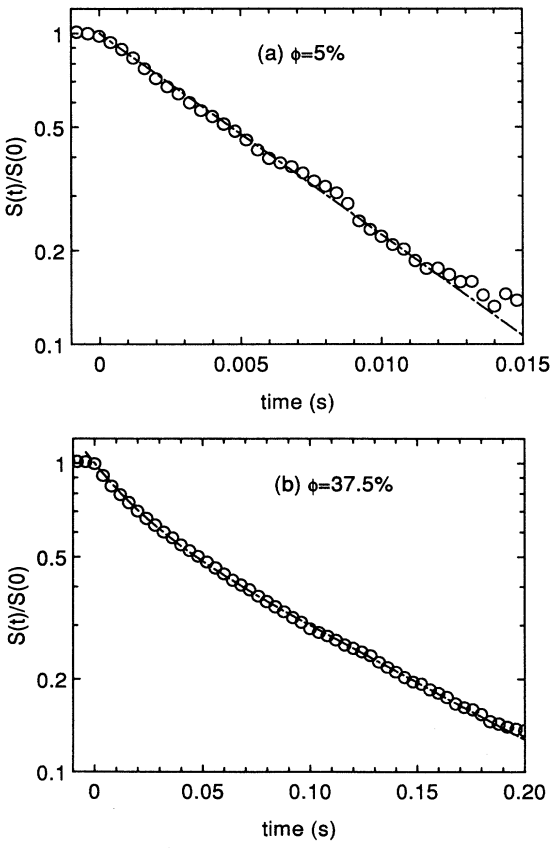

FIG. 6. Semilog plot of the orientational order parameter versus time for (a) $\phi = 5$ and (b) 37.5% suspensions of 2.4:1 AR PTFE. The dashed lines are the best fits of Eq. (13) to the data.

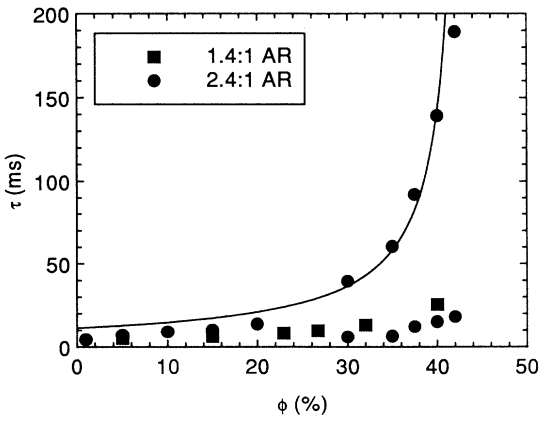

FIG. 7. Relaxation times versus concentration for the 2.4:1 and 1.4:1 AR PTFE samples. The solid line is a fit of Eq. (14) to the slow relaxation time data for the 2.4:1 AR data.

cally in agreement with the model presented in Sec. II, but the critical increase of the order parameter, which is predicted to accompany the increase in relaxation time, is not observed at any intensity parameter for concentrations that are close to the critical concentration m_c for the isotropic-nematic phase transition. We present the following possible explanation for these results. In the course of developing a theoretical model for AAKM, it was assumed that the optical axis for the particles was colinear with the long (geometrical) axis of the particles. If this is not true, then a single order parameter is not sufficient to describe the orientational order of the suspension. In that case, two order parameters should be introduced: one "S," which characterizes the orientation of the optical axis **j**, and another "Q," which characterizes the orientation of the long axis $\boldsymbol{l}$. These may be written

$$S=\tfrac{3}{2}\langle\cos^2\theta_j-\tfrac{1}{3}\rangle\ ,$$
$$Q=\tfrac{3}{2}\langle\cos^2\theta_l-\tfrac{1}{3}\rangle\ , \tag{15}$$

where θ_j and θ_l are the angles made by the optical and geometrical axes of the particle and the direction of the applied electric field $\hat{e}_z$, respectively. Note that it is the optical order parameter S that is measured in both of the experiments described above. The potential energy of the microparticles due to the E field and the excluded volume effect follow from Eqs. (3) and (4):

$$U_E=-\frac{\beta}{2}\bar{E}^2\cos^2\theta_j\ ,$$
$$U_{\rm ex}=-\tfrac{3}{2}mk_BT(\cos^2\theta_l-\tfrac{1}{3})Q\ . \tag{16}$$

Using Eqs. (16) and (2) for the orientational distribution function, we obtain by analogy with Eq. (5) two coupled equations for Q and S. For small enough fields, and when $m<m_c$, we can use the linear approximation, which gives

$$S=\tfrac{2}{15}J+\frac{m}{m^*}f(\gamma)Q\ ,$$
$$Q=\tfrac{2}{15}Jf(\gamma)+\frac{m}{m^*}Q\ , \tag{17}$$

where γ is the angle between **j** and $\boldsymbol{l}$ and

$$f(\gamma)=\tfrac{15}{4}\langle\cos^2\theta_j(3\cos^2\theta_l-1)\rangle\ . \tag{18}$$

The solution of Eq. (17) for S and Q is

$$S=\tfrac{2}{15}J\left[1+\frac{m}{m^*}\frac{f^2}{1-m/m^*}\right]$$
$$Q=\tfrac{2}{15}J\frac{f}{1-m/m^*}\ . \tag{19}$$

The numerical values of $f(\gamma)$ are plotted in Fig. 8. It is seen that as γ increases, $f(\gamma)$ decreases, causing S to decrease. Using the values of $S=0.06$, $J=0.3$ measured in the optical Kerr experiment for the $\phi=40\%$ suspension [see Fig. 4(a)], and estimating the concentration of this sample to correspond to $m=4$, the value of γ, which is calculated using the optical order parameter written in Eq. (19) and Fig. 8, is $\gamma=39°$. This value seems reasonable in light of a transmission electron microscopy study carried out on samples of similarly prepared PTFE suspensions [20]. In that work, electron-diffraction patterns from single PTFE microparticles with AR of roughly 2:1 or less are arcs that subtend angles of up to 45°. That result indicates that the microparticles are in fact polycrystalline, and that the distribution of individual domains within a single particle range over 45°. Based on this observation, it seems reasonable to assert that the net optical axis need not coincide with the geometrical axis of the microparticles. This point of view is also supported in Ref. [21], where further experimental evidence is presented, suggesting that the internal structure of similarly prepared PTFE particles is somewhat irregular.

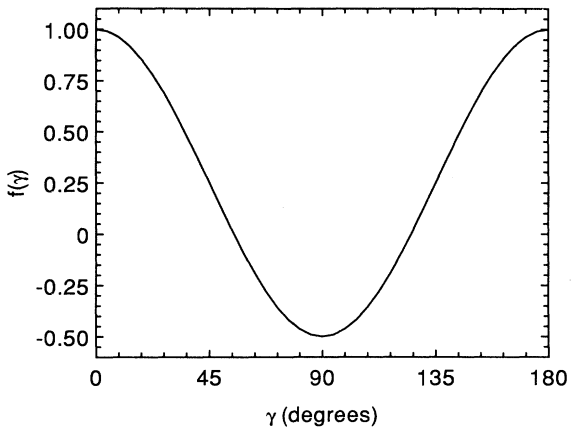

FIG. 8. The function f versus γ, where γ is the angle between the geometrical and the optical axes of a shaped, dielectric microparticle.

The observation that the decay of the orientational order parameter for PTFE at high concentrations is not a single exponential can be shown as well to be an indication that the optical and geometrical axes are not colinear. By analogy with Eq. (7), the dynamical equations that are satisfied by the two order parameters assume the following form in the linear approximation:

$$\frac{dS}{dt}=-\frac{1}{\tau}\left[S-\frac{2}{15}J-\frac{m}{m^*}fQ\right]\ ,$$
$$\frac{dQ}{dt}=-\frac{1}{\tau}\left[Q-\frac{2}{15}Jf-\frac{m}{m^*}Q\right]\ . \tag{20}$$

These two equations are solved for $t>0$ by setting $J=0$ (fields turned off at $t=0$) and using Eqs. (19) as the initial conditions $S(0)$ and $Q(0)$. This yields the following expression for the optical order parameter:

$$S(t)=S(0)\left[\frac{(1-m/m^*)(1-f^2)}{1-(m/m^*)(1-f^2)}e^{-t/\tau}+\frac{f^2}{1-(m/m^*)(1-f^2)}e^{-t/\tau^*}\right]\ , \tag{21}$$

where τ^* is given by Eq. (9). Using the experimentally determined value of $c_s=0.826$ and an estimate of $m=4$

for the higher concentrations used in the optical Kerr experiment, the value of γ calculated from Eq. (21) and Fig. 8 is $\gamma = 27°$. This value is in reasonable agreement with the value determined from the measurement of the magnitude of the optical order parameter and is within the range suggested by the results of Ref. [20].

V. CONCLUSIONS

In summary, we have studied the concentrational effects on the orientational ordering of shaped AAKM and found that the expected pretransitional behavior of the orientational order parameter in PTFE suspensions was suppressed, and the relaxation of orientational ordering does not decay exponentially. We have shown that these results can be explained if the optical and geometrical axes of the PTFE microparticles are not colinear.

ACKNOWLEDGMENTS

The authors acknowledge the skillful assistance of Colleen Stevens in performing experiments in the preliminary stages of this work, and Yue Hu for her helpful comments concerning the construction of the cell electrodes used in the electric birefringence experiment.

[1] D. Rogovin, J. Scholl, R. Pizzoferrato, M. DeSpirito, M. Marinelli, and U. Zammit, J. Opt. Soc. Am. B **8**, 2370 (1991).

[2] R. Pizzoferrato, M. DeSpirito, U. Zammit, M. Marinelli, F. Scudieri, and S. Martelucci, Phys. Rev. A **41**, 2882 (1990).

[3] D. Rogovin, J. Scholl, R. Pizzoferrato, M. DeSpirito, U. Zammit, and M. Marinelli, Phys. Rev. A **44**, 7580 (1991).

[4] R. Pizzoferrato, D. Rogovin, and J. Scholl, Opt. Lett. **16**, 297 (1991).

[5] P. G. deGennes and J. Prost, *The Physics of Liquid Crystals,* 2nd ed. (Clarendon, Oxford, 1993).

[6] Chaohua Wang, B. E. Vugmeister, and H. Daniel Ou-Yang, Phys. Rev. E **48**, 4455 (1993).

[7] Boris E. Vugmeister, Michelle S. Malcuit, John C. Kralik, and Colleen Stevens, in *Electrical, Optical, and Magnetic Properties of Organic Solid State Materials,* MRS Symposia Proceedings No. 328 (Materials Research Society, Pittsburgh, 1994), pp. 619–624.

[8] M. Doi and S. F. Edwards, *The Theory of Polymer Dynamics* (Clarendon, Oxford, 1986), pp. 303 and 304.

[9] H. See, M. Doi, and R. Larson, J. Chem. Phys. **92**, 792 (1990).

[10] M. DeSpirito, R. Pizzoferrato, M. Marinelli, U. Zammit, D. Rogovin, R. McGraw, and J. Scholl, Opt. Lett. **16**, 120 (1991).

[11] For a summary of the applications of thermotropic liquid crystals to nonlinear optics, see Iam Choon Khoo, *Progress in Optics XXVI,* edited by E. Wolf (Elsevier Science, New York, 1988), pp. 105–161.

[12] ALGOFLON D60/A, kindly supplied by Ausimont USA, Inc., Morristown, NJ.

[13] FLUON AD-1, kindly supplied by ICI Fluoropolymers Division, Exton, PA.

[14] M. DeSpirito, R. Pizzoferrato, U. Zammit, M. Marinelli, F. Scudieri, S. Martellucci, and M. Romagnoli, Opt. Lett. **14**, 239 (1989).

[15] R. Piazza, J. Stavans, T. Bellini, and V. Degiorgio, Opt. Commun. **73**, 263 (1989).

[16] F. W. Billmeyer, Jr., J. Appl. Phys. **18**, 431 (1947).

[17] Cheser T. O'Konski and Sonja Krause, in *Molecular Electro-Optics,* edited by Chester T. O'Konski (Dekker, New York, 1976), Pt. 1, pp. 63–120.

[18] Yue Hu, J. L. Glass, A. E. Griffith, and Seth Fraden, J. Chem. Phys. **100**, 4674 (1994).

[19] T. Bellini, R. Piazza, C. Sozzi, and V. Degiorgio, Europhys. Lett. **7**, 561 (1988).

[20] Henri D. Chanzy, Paul Smith, and Jean-Francois Revol, J. Polym. Sci. Polym. Lett. Ed. **24**, 557 (1986).

[21] Forrest J. Rahl, Michael A. Evanco, Robert J. Fredericks, and Annemarie C. Reimschuessel, J. Polym. Sci. Part A **10**, 1337 (1972).